ACACIA

Advancing the Science for Aviation and Climate

ACACIA

Deliverable 2.5

Title: Report or publication on satellite assessment of aviation impact on cirrus

Lead partner: ULEI

Project no.	875036
Instrument	Research and Innovation Action (RIA)
Thematic Priority:	H2020-MG-2018-2019-2020
Start date of project:	1 January 2020
Duration:	42 months
Date of report:	20 June 2022
Document authors:	Johannes Quaas
Classification:	PU (Public)
File name:	ACACIA-Deliverable D2.5.pdf

TABLE OF CONTENTS

1 Summary

One of the main goals in ACACIA studying the impact of aviation on cirrus was to derive insights from satellite analysis that may now be tested using models. This was addressed by two approaches: on the one hand, an assessment of the integral effect of aviation on cirrus coverage and emissivity was aimed at. On the other hand, a detailed microphysical study was conducted.

Quaas et al. (2021) exploited the fact that during the COVID-19 pandemic, passenger air traffic was shut down to a large extent. Comparing boreal spring 2020 with strongly reduced air traffic to the preceding years, it was found that 17% of all cirrus are due to air traffic, in the regions with large traffic (20% of the area in the Northern hemisphere mid-latitudes). This translates into an estimated forcing of 61 mW m^{-2}. This result corroborates, from satellite observations, the assessment e.g. by the latest IPCC report which, however, largely relied on modelling only.

Subsequently, Marjani et al. (2022) conducted a detailed study investigating cirrus after specific aircraft passages intersecting the satellite lidar / radar track. The study aimed at identifying the microphysical perturbation towards a better process understanding on the cirrus enhancement by air traffic. The key result was that ice crystal number concentration is enhanced by about 50% beneath the aircraft.

In the next step in ACACIA, these observational results are now explored using atmospheric cloud-resolving modelling.

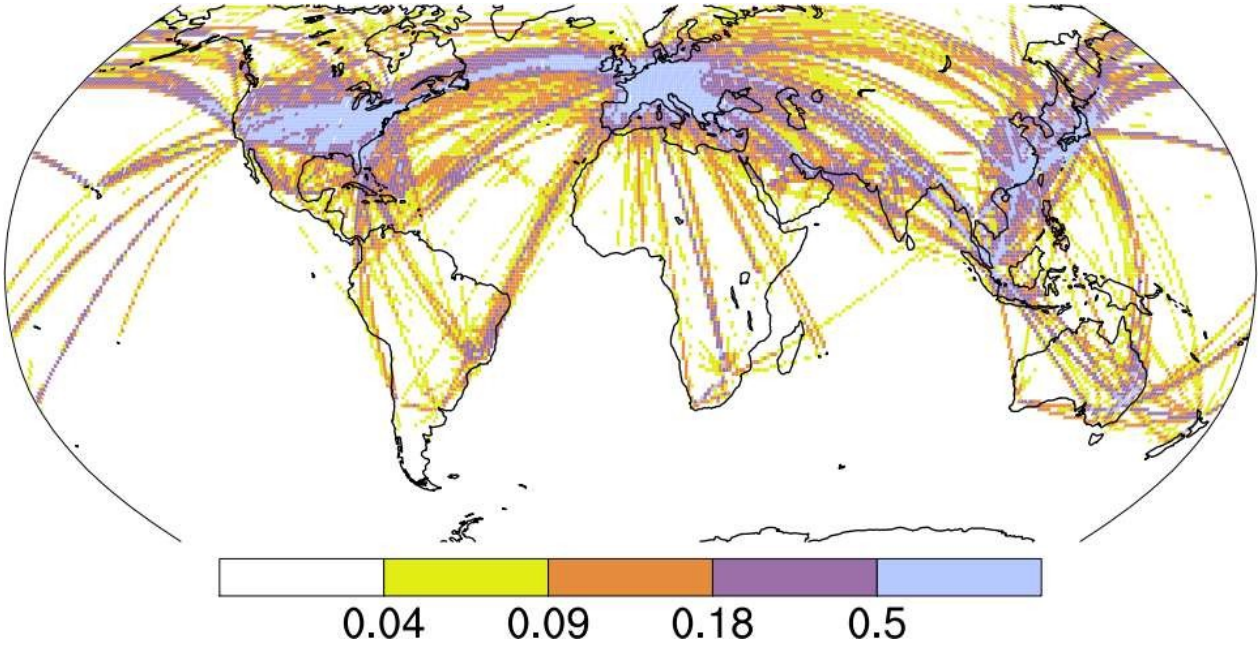

Figure 1: Difference in flight track density [km km^{-2} day^{-1}] March – May 2019 minus March – May 2020. The colour scale corresponds to the five quintiles shown in the x-axis of in Figs. 2 and 3.

2 Satellite-derived assessment of the aviation-cirrus climate effect

2.1 Abstract of the publication

Aircraft produce condensation trails, which are thought to increase high-level cloudiness under certain conditions. However the magnitude of such an effect and whether this contributes substantially to the radiative forcing due to the aviation sector remain uncertain. The very substantial, near-global reduction in air traffic in response to the COVID-19 outbreak offers an unprecedented opportunity to identify the anthropogenic contribution to the observed cirrus coverage and thickness. Here we show, using an analysis of satellite observations for the period March–May 2020, that in the 20% of the Northern Hemisphere mid-latitudes with the largest air traffic reduction, cirrus fraction was reduced by ∼9 ± 1.5% on average, and cirrus emissivity was reduced by ∼2 ± 5% relative to what they should have been with normal air traffic. The changes are corroborated by a consistent estimate based on linear trends over the period 2011–2019. The change in cirrus translates to a global radiative forcing of 61 ± 39 mW m^{-2}. This estimate is somewhat smaller than previous assessments.

2.2 Summary of the key results

The idea of the study was to exploit the aviation shutdown during the COVID-19 pandemic. The aviation activitiy was computed using FlightRadar24 data, that demonstrated decreases by about 70% in large parts of the Northern hemisphere mid-latitudes (Fig. 1). For the regions with large decrease in flight activitiy, satellite-derived cirrus occurrence and emissivity from the MODerate Resolution Imaging Spectroradiometer (Platnick et al., 2017) were analysed for the boreal spring 2020 period (March-April-Mai, MAM). In order to account for differences in weather conditions, circulation analogues were computed for each region and day of the time period using pattern correlation of the 500-hPa geopotential pattern. In order to simplify the analysis and to improve the signal-to-noise ratio, the entire Northern hemisphere mid-latitudes were distinguished into five quintiles of air traffic change (Fig. 1). The cirrus

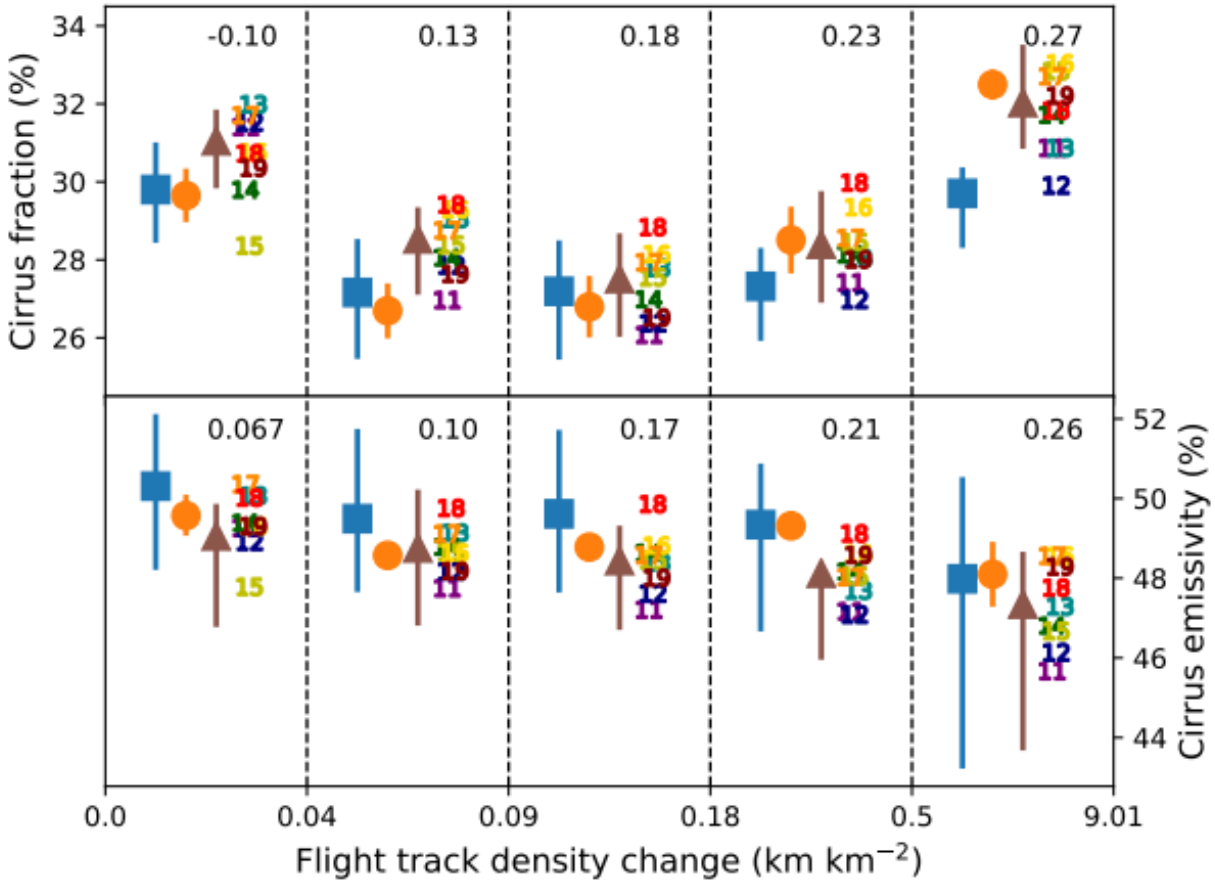

2021:Figure 2: Cirrus fraction and emissivity as a function of flight track density change between 2020 and 2019 increases in the midlatitudes of the Northern Hemisphere. Cirrus fraction (top) and emissivity (bottom) from daily level-3 (1°x 1°) MODIS retrievals, both expressed in percent, as a function of quintiles of the difference in flight track density, for grid-boxes containing cirrus. The mean of the spatio-temporal distribution of the 1° x 1° grid-boxes in the region 27° to 68°N is shown. Both MODIS-Terra (approximate overpass times 10.30 a.m. and 10.30 p.m.) and MODIS-Aqua (overpass times 1.30 a.m. / 1.30 p.m.) data are considered. Blue squares – March-May 2020; orange circles – circulation analogues March-May 2011–2019; brown triangles – climatology March-May 2011–2019. Also the March – May means for each year, averaged for all four satellite overpasses, are provided, colour coded from purple (2011 marked as 11) to dark red (2019 marked as 19). The numbers in the top right for each quintile show the linear trends 2011 – 2019 (% year^{-1}), as absolute percent changes. The vertical bars show the range spanned by the four satellite overpass times.

coverage and emissivity was computed in each of the quintiles (a) for MAM 2020; (b) for the MAM climatology 2011 – 2019 and (c) for the circulation analogues during this period. The results are shown in Fig. 2. It is seen that also for regions with little air traffic change, MAM 2020 was different from the climatology, but close to the circulation analogues, i.e. weather did play a role. For the two quintiles with large air traffic change, a distinct signal is found. It is also evident in Fig. 2 that there is a substantial trend in cirrus coverage between 2011 and 2019. The differences are shown in Fig. 3. In particular the cirrus coverage was changed, by 9.1% absolute in the quintile with the largest air traffic reduction, 4.7% in the next-largest. Emissivity, in turn, changed to a lesser extent.

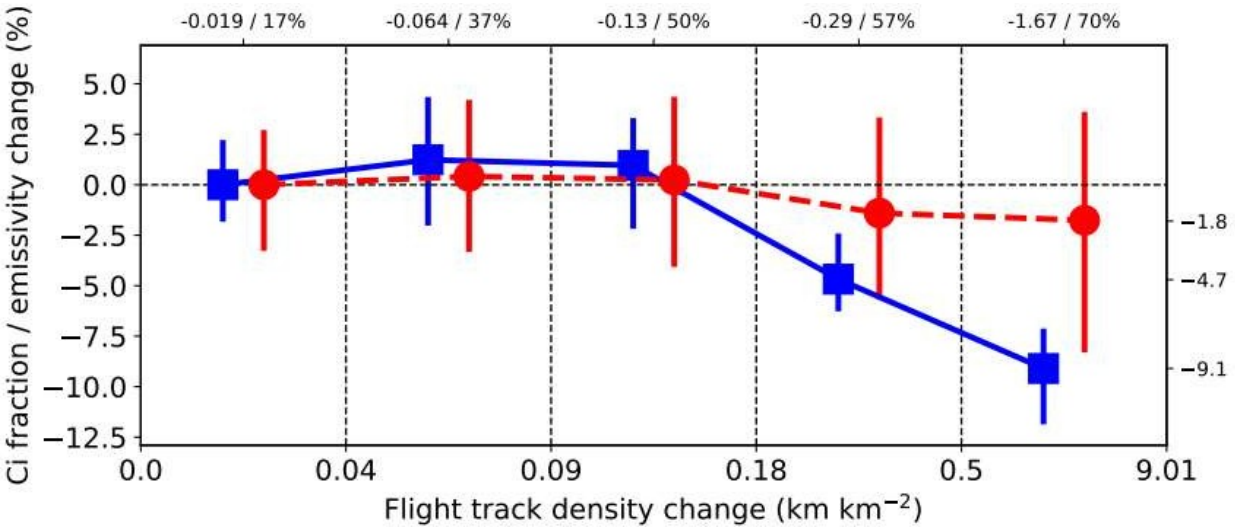

Figure 3: Cirrus fraction and emissivity decrease as flight track density change increases when computed for similar weather conditions. Mean relative difference in cirrus fraction (blue squares) and cirrus emissivity (red circles) between March–May 2020 and March–May in analogue circulations 2011–2019, expressed as the deviation from zero aviation change (lowest quintile), as a function of flight track density change 2019 minus 2020. The vertical bars show the full range spanned by the four satellite overpasses. The labels on the top indicate the average change in flight track density within each quintile in absolute and in relative numbers.

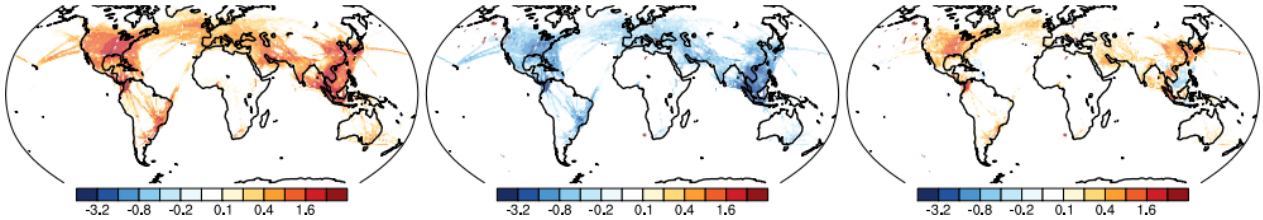

Figure 4: Radiative forcing (Wm^{-2}) due to aviation-induced cirrus in March–May 2019. Left: terrestrial (longwave) spectrum, middle: solar (shortwave spectrum), right: net radiative forcing.

Fig. 4 translates these changes into radiative forcing numbers, computed using the weather conditions of 2019 and the change with respect to 2019. These are scaled considering the air traffic change in the control period and also the fact that air traffic did not shut down entirely in 2020. The overall result is a forcing of 61±39 mW m^{-2} for 2019, indeed rather close to the mostly model-based estimates of Lee et al. (2021) and Forster et al. (2022) who obtained 57 and 60 mW m^{-2}, respectively.

3 Satellite analysis of the microphysical perturbation of cirrus

3.1 Abstract of the publication

Contrails can persist in cloud-free supersaturated air, increasing high-cloud cover, and inside natural cirrus cloud, modifying the microphysical properties of them. The latter effect is almost unknown, partly because of the lack of height-resolved measurements and the capability of measurements to penetrate inside the cloud. New retrievals of the ice crystal number concentration from combined satellite cloud radar and lidar measurements (CloudSat/CALIPSO; DARDAR-Nice algorithm) now allow for satellite-based assessment inside the clouds. We investigate this issue at intersections between the aircraft flight tracks and these retrieval profiles. Regions behind the aircraft inside the flight track were compared to the adjacent regions and to ahead of the aircraft, along the satellites' profiles, where DARDAR-Nice identify geometrically thin cirrus clouds. This comparison revealed a statistically significant increase of 25% and 54% in the concentration of ice crystals with the minimum size of 5 μm around 300–540-m beneath an aircraft's flight altitude.

3.2 Summary of the key results

Following an earli.er study by Tesche et al. (2016) who investigated normalized cloud optical depth, Marjani et al. (2022) now were able to investiage microphysical details of changes in cirrus. This is thanks to a new satellite retrieval of the ice crystal number concentration on the basis of the CALIPSO satellite cloud lidar and the CloudSat satellite cloud radar in the lidar-radar (DARDAR) retrieval by Sourdeval et al. (2018).

The key result is shown in Fig. 5: behind an aircraft passage intersecting the CALIPSO-CloudSat track, ice crystal number concentration is enhanced by up to about 54% beneath the aircraft.

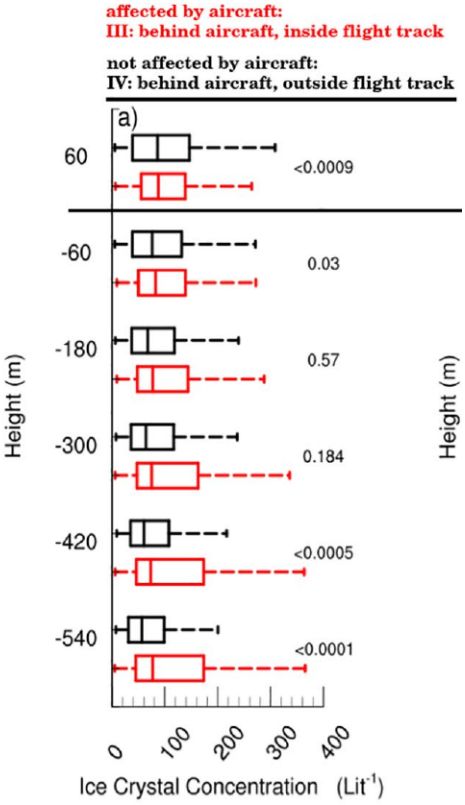

Figure 5: DARDAR-Nice ice crystal number concentration as a function of height as summary statistics over all cases.Centered 3-point moving average values over 60-m intervals of height levels are used to produce box-whisker diagrams.Vertical axis represents height relative to the aircraft altitude. Boxes show the 25th–75th percentiles of the data, whiskersthe 5th–95th percentiles; the middle bar is the median value. In both panels, the red boxes are the same, namely category III(behind the aircraft, inside flight track). In (a), the black boxes are category IV (behind the aircraft, outside the flight track),in (b) category I (ahead the aircraft, inside the flight track), i.e., two different choices for the control case. Two-tailed p-valuescalculated from t-score are indicated in right-hand side of each height level. If the p-value is less than the significance level of 0.05, the null hypothesis is rejected (i.e., aviation do have effect on already existing cirrus).

4 References

Lee, D. S., D. W. Fahey, A. Skowron, M. R. Allen, U. Burkhardt, Q. Chen, S. J. Doherty, S. Freeman, P. M. Forster, J. Fuglestvedt, A. Gettelman, R. R. De León, L. L. Lim, M. T. Lund, R. J. Millar, B. Owen, J. E. Penner, G. Pitari, M. J. Prather, R. Sausen, and L. J. Wilcox, The contribution of global aviation to anthropogenic climate forcing for 2000 to 2018, Atmos. Environ., 244, 1-29, doi:10.1016/j.atmosenv.2020.117834, 2021.

Forster, P., T. Storelvmo, K. Armour, W. Collins, J.-L. Dufresne, D. Frame, D.J. Lunt, T. Mauritsen, M.D. Palmer, M. Watanabe, M. Wild, and H. Zhang, The Earth's Energy Budget, Climate Feedbacks, and Climate Sensitivity. In Climate Change 2021: The Physical Science Basis. Contribution of Working Group I to the Sixth Assessment Report of the Intergovernmental Panel on Climate Change [Masson-Delmotte, V., P. Zhai, A. Pirani, S.L. Connors, C. Péan, S. Berger, N. Caud, Y. Chen, L. Goldfarb, M.I. Gomis, M. Huang, K. Leitzell, E. Lonnoy, J.B.R. Matthews, T.K. Maycock, T. Waterfield, O. Yelekçi, R. Yu, and B. Zhou (eds.)]. Cambridge University Press, Cambridge, United Kingdom and New York, NY, USA, pp. 923–1054, doi:10.1017/9781009157896.009, 2021.

Marjani, S., M. Tesche, P. Bräuer, O. Sourdeval, and J. Quaas, Satellite observations of the impact of aviation on ice crystal number in cirrus clouds, Geophys. Res. Lett., 49, e2021GL096173, doi:10.1029/2021GL096173, 2022.

Platnick, S., et al., The MODIS cloud optical and microphysical products: Collection 6 updates and examples from Terra and Aqua, IEEE Transact. Geosci. Remote Sens. 55, 502–525, doi:10.1109/TGRS.2016.2610522, 2017.

Quaas, J., E. Gryspeerdt, R. Vautard, and O. Boucher, Climate impact of aircraft-induced cirrus assessed from satellite observations before and during COVID-19, Environ. Res. Lett., 16, 064051, doi:10.1088/1748-9326/abf686, 2021.

Sourdeval, O., E. Gryspeerdt, M. Krämer, T. Goren, J. Delanoë, A. Afchine, F. Hemmer, and J. Quaas, Ice crystal number concentration estimates from lidar-radar satellite remote sensing. Part 1: Method and evaluation, Atmos. Chem. Phys., 18, 14327-14350, doi:10.5194/acp-18-14327-2018, 2018.

Tesche, M., P. Achtert, P. Glantz, and K. J. Noone, Aviation effects on already-existing cirrus clouds, Nature Comm. 7, 12016, doi: 10.1038/ncomms12016, 2016.